ISSN 1674-1056
http://cpb.iphy.ac.cn
http://iopscience.iop.org/cpb
中国物理 B
Chinese Physics
中国物理
Chinese Physics B

Avalanching patterns of irregular sand particles in continual discrete flow

Ren Han(韩韧), Yu-Feng Zhang(张宇峰), Ran Li(李然), Quan Chen(陈泉), Jing-Yu Feng(冯靖禹), Ping Kong(孔平)
Citation: Chin. Phys. B . 2020, 29(2): 024501 . **doi:** 10.1088/1674-1056/ab65b8
Journal homepage: http://cpb.iphy.ac.cn; http://iopscience.iop.org/cpb

What follows is a list of articles you may be interested in

Experimental and numerical study on energy dissipation in freely cooling granular gases under microgravity

Wen-Guang Wang(王文广), Mei-Ying Hou(厚美瑛), Ke Chen(陈科), Pei-Dong Yu(虞培东), Matthias Sperl
Chin. Phys. B . 2018, 27(8): 084501 . **doi:** 10.1088/1674-1056/27/8/084501

The anisotropy of free path in a vibro-fluidized granular gas

Yifeng Mei(梅一枫), Yanpei Chen(陈延佩), Wei Wang(王维), Meiying Hou(厚美瑛)
Chin. Phys. B . 2016, 25(8): 084501 . **doi:** 10.1088/1674-1056/25/8/084501

Avalanching patterns of irregular sand particles in continual discrete flow*

Ren Han(韩韧)[1], Yu-Feng Zhang(张宇峰)[1], Ran Li(李然)[2], Quan Chen(陈泉)[1], Jing-Yu Feng(冯靖禹)[1], and Ping Kong(孔平)[3,†]

[1] School of Optical-Electrical and Computer Engineering, University of Shanghai for Science and Technology, Shanghai 200093, China
[2] School of Medical Instrument and Food Engineering, University of Shanghai for Science and Technology, Shanghai 200093, China
[3] Shanghai Key Laboratory for Molecular Imaging, Department of Science and Liberal Art, Shanghai University of Medicine and Health Sciences, Shanghai 201318, China

(Received 21 October 2019; revised manuscript received 9 November 2019; accepted manuscript online 27 December 2019)

We investigate the flow patterns of irregular sand particles under avalanching mode in a rotating drum by using the spatial filtering velocimetry technique. By exploring the variations of velocity distribution of granular flow, we find a type of avalanching pattern of irregular sand particles which is similar to that of spherical particles flow. Due to the fact that the initial position of avalanche in this pattern locates at the middle of the drum and the avalanche propagates toward the edge area gradually, we named it as mid-to-edge avalanching pattern. Furthermore, we find another avalanching pattern which slumps from the edge and propagates toward the opposite edge of the flow surface, named as edge-to-edge pattern. By analyzing the temporal and spatial characteristics of these two types of avalanching patterns, we discover that these two types of avalanche patterns are caused by that the avalanching particles constantly perturb the axial adjacent particles. Thus, the particles on the flow surface are involved in avalanching sequentially in order of the axial distance from the initial position.

Keywords: spatial filtering velocimetry (SFV) method, avalanching pattern, velocity distribution, irregular particles

PACS: 45.70.Ht, 45.70.Mg, 43.58.Fm **DOI:** 10.1088/1674-1056/ab65b8

1. Introduction

Dynamic characteristics of granular materials in rotating drum is an attractive topic, and avalanche, as a distinct dynamic behavior of granular material, captures much attention among the researchers.[1–4] Understanding avalanche of granular material is beneficial to the prevention of natural disasters, such as mudslides or landslides. On the other hand, research achievements on avalanche can be widely used in chemical, mineral, ceramic, pharmaceutical, and food processing fields. In addition, as the particle shape has a significant influence on granular dynamics, the avalanches for irregular particles have more complex and unique characteristics compared to the spherical particles.[5–14] Adrian *et al.*[15] investigated single avalanches created by perturbing a static layer of glass beads on a rough inclined plane. The authors observed two types of avalanching behavior with the increasing of the inclined angle. The difference between the two types mainly is whether there exits a uphill propagation of the avalanche. Jean[16] investigated the nucleation and the growth of avalanches in a rotating drum and further analyzed the propagating velocity of the avalanche in the radial direction. Yang *et al.*[17,18] studied the velocity distribution of the glass sand in the rotating drum. The authors declared that there exits particle accumulation in the central position of the avalanche surface and no similar phenomenon is observed for regular particles. The irregular particle accumulation clearly affects the dynamic characteristics of the particulate flow in both axial and radial directions. Although there have been some achievements in the study of the avalanching of irregular particles, the scope is still relatively limited. Therefore, this paper further explores the avalanching pattern of irregular particles along the axial direction in rotating drum based on the work mentioned above.

Spatial filtering velocimetry (SFV) method is an effective velocity measurement method which shows advantages in precision, stability, and usability compared to other common methods. Gong *et al.*[19] first applied SFV method to measure velocity of particles flow in the rotating drum and proved that the method is suitable for this application. Lin *et al.*[20] used the SFV method to measure the velocity of particles in the rolling regime. The authors found that there exist two peak velocities for irregular particles in the case of low rotating speed and the two peak velocities gradually merge into one peak velocity with the increasing of rotating speed which is significantly different from always one peak velocity for the regular particles. But the work mainly concentrated on the center region of particle surface in the drum, and the velocity distributions over entire particle surface are expected to be explored.

*Project supported by the National Natural Science Foundation of China (Grant Nos. 11572201, 91634202, and 11902190).
†Corresponding author. E-mail: kongp@sumhs.edu
© 2020 Chinese Physical Society and IOP Publishing Ltd

In this paper, the avalanching characteristics of the irregular sand particles flow in rotating drum is further studied by SFV method. After a section on the experimental setup and method, we first analyze in the results and discussion section the variations of velocity distribution of granular flow and then present two types of avalanche patterns which named as mid-to-edge pattern and edge-to-edge pattern respectively. Moreover, the temporal and spatial characteristics of these two types of avalanching patterns are explored in the results and discussion section.

2. Experimental setup and method

2.1. Experimental setup

As shown in Fig. 1, the experimental system mainly consists of a rotating drum, an LED light, and a CCD camera. The rotating drum is made of transparent plexiglas with a diameter and length of 150 mm and 200 mm respectively. A high-precision DC motor is used to control the rotating speed of the drum which is set to 3.5 RPM in this experiment. The irregular granular materials filled in the drum are glass sand particles with effective particle size in the range of 1 mm–1.5 mm, which are classified as sub-angular particles. The irregular glass sand is characterized with equivalent projected area diameter of 1.30 ± 0.17 mm, the corresponding sphericity is around 0.87, the aspect ratio is 0.69, and the convexity is 0.96. In this experiment, the filling degree of glass sand particles is set to 40% in the drum.

The experimental system employs a light source (white LED) and detector (linear CCD camera) for collecting experimental data. As shown in Fig. 1(b), the CCD camera is mounted on a metal bracket and its shooting angle is adjusted to be perpendicular to the surface of particulate flow which is the rectangular area surrounded by red lines. In order to facilitate the data analysis, we use X and Y to indicate the axial and radial directions on the surface of particulate flow respectively. Due to the particularity of the irregular particle shape, the surface of the particulate flow in our experiment is not completely flat. Meanwhile, the inclination of the surface particle flow is always changing during the avalanche. If the surface of the detector is not absolutely parallel to the particulate flow and we assume that the error angle between them is θ, there must be a difference between the velocity directions of the surface of the particulate flow V and linear CCD pixels array, and the velocity measured by the experiment is $V' = V \cdot \cos\theta$. Therefore, the measurement error is $\Delta V = V \cdot (1 - \cos\theta)$. In this case, the angular difference is controlled within 10°. Consequently, the systematic error of the measurement result is less than 1.5% which is acceptable in the measurement as the validation study with conveyor belt has error within 3% (average 1.5%) in our previous paper.[19] The sampling frequency of linear CCD camera is set to 1000 Hz, and the experimental data are transported to the host computer through the Ethernet interface.

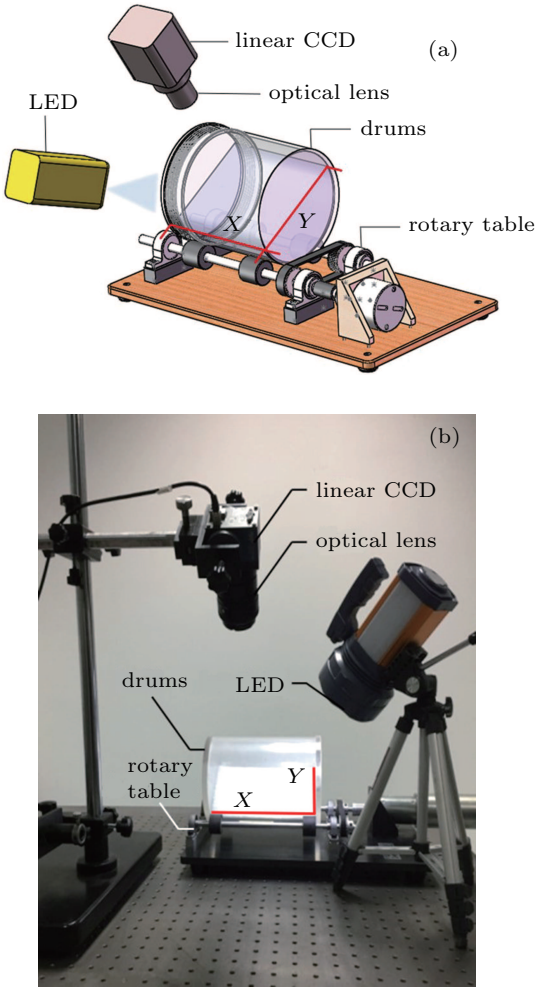


Fig. 1. Particle velocity measurement system based on SFV method. (a) Schematic diagram and (b) image of experimental setup.

2.2. The SFV method

SFV is an effective method for measuring the velocity of moving object based on analyzing the images of the object when going through a parallel slit or a transmission grating.[21–23] When the light source irradiates the surface of the moving object with speed v, the rough surface of the object leads to a light scattering phenomenon. A part of scattering light passes through the objective lens and images on the spatial filter composed of the grating, then the light passing through the grating is focused by the lens and received by the photoelectric sensor. Due to the narrow bandpass filtering characteristics of the spatial slit, the scattered light signal containing the velocity information of the moving object can be received by the photoelectric sensor through the spatial slit, and the photoelectric sensor outputs the varying sinusoidal signals.[24–33] Since the measured object has a sustained velocity v and the grating has a spatial period length p, the output signal of photoelectric sensor can achieve a stable period $T_0 = p/v$.

According to the relationship between the period of the signal and the frequency $f_0 = 1/T_0$, the velocity of the measured object can be calculated by the following equation:[31]

$$v_0 = \frac{p \cdot f_0}{M},$$

where M is the magnification of the optical system.

2.3. Avalanching pattern for spherical particles

The avalanching pattern of spherical particles is an attractive topic and often studied by using the inclined plane and the rotating drum. In order to explore the avalanching pattern of spherical particles on the inclined plane, we pour spherical particles abundantly at the top of the plane by setting a suitable angle. The moving particles leave behind a static layer of uniform thickness. An initial position of the avalanche will occur onto this layer if we add some extra beads. Then the avalanche propagates to the surroundings until the edges of the layer which is also mentioned by Adrian.[15] In addition, the avalanching pattern of spherical particles in rotating drum also satisfies this rule and the upper front is shown to propagate upwards with a velocity which is equal to the averaged velocity of the flowing grains, whereas the velocity of the downslope propagating front is approximately equal to twice the avalanche velocity which is also concluded by Jean.[16]

3. Results and discussion

3.1. Mid-to-edge pattern

Mid-to-edge pattern is an interesting type of avalanching pattern similar to the spherical particles. By means of measuring the velocity distribution of the surface particulate flow, we observe the propagation process of the avalanche in mid-to-edge pattern. In order to elaborate the avalanching pattern, we use the term high-speed area to indicate the region where there are the highest velocities of surface particulate flow and labeled as H1, H2, and H3 respectively in Fig. 2. That is the avalanche in high-speed area is most intense. As shown in Fig. 2(a), the initial position occurs at the center of the drum, and expand toward the edge area gradually in the middle stage (as shown in Fig. 2(b)). Finally, the high-speed area arrives at the edges of the drum which indicates that the avalanche is about to end (shown in Fig. 2(c)). What the high-speed area continuously expands toward both sides of the drum indicates the propagation of the avalanche along the axial direction. An interpretation for the phenomena is that the particles in the high-speed area repeatedly perturb the surrounding particles and especially make the axially adjacent particles in avalanche sequentially.

In order to describe the mid-to-edge pattern in a more further detail, we make quantitative studies on spatial and temporal distributions of the velocity of the surface particulate flow respectively. Firstly, the temporal distribution of the velocity is considered. As shown in Fig. 3, a banded area marked by black dotted line is selected and five sampling areas are set up which are labeled as A1–A5 in the banded area. The size of all the sampling areas in this paper is uniformly set to 22 mm×16 mm. Meanwhile, the avalanche period is divided into 10 slices and the velocities of surface particulate flow in A1–A5 for each of these slices are measured by using SFV method.

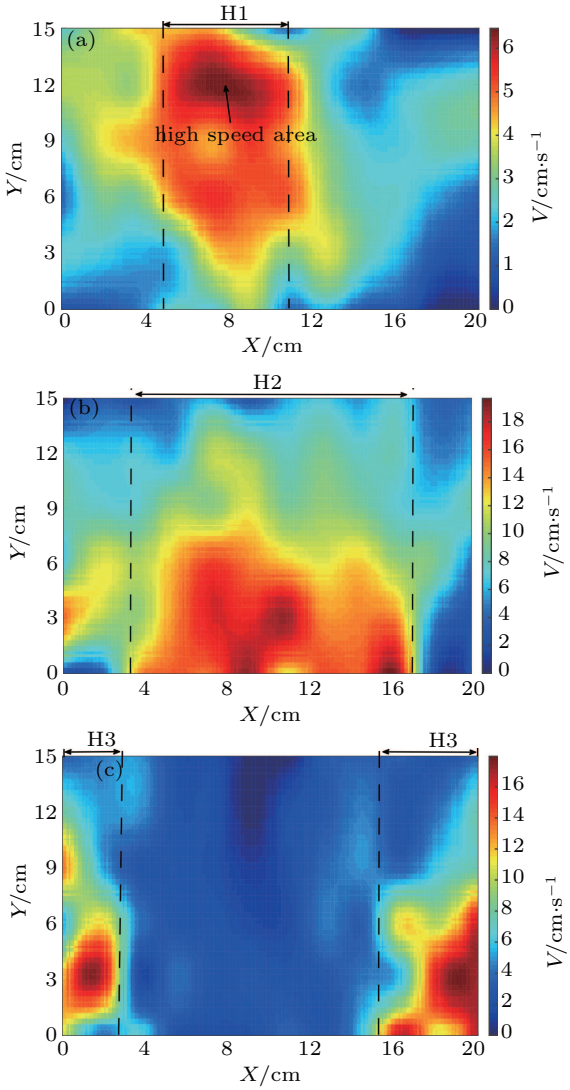


Fig. 2. The velocity distribution of the surface particulate flow in mid-to-edge pattern. (a) The velocity distribution at the initial stage, (b) the velocity distribution at the middle stage, and (c) the velocity distribution at the end stage of the avalanche.

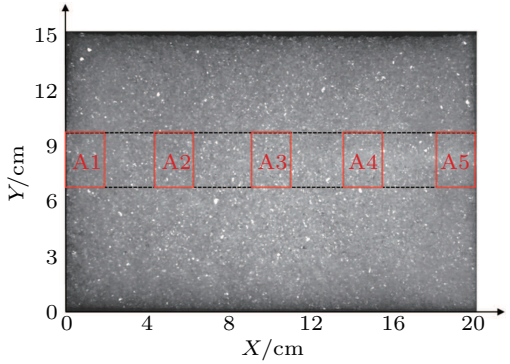


Fig. 3. The schematic diagram of sampling area.

According to the mid-to-edge pattern shown in Fig. 2, the avalanche propagates from the central region to both sides of the drum, so we choose the central region (A3) and edge regions (A1 and A5) to explore the variation of the velocity of the surface particulate during the avalanche procedure. We achieve the temporal distribution of the velocity in the mid-to-edge pattern which is displayed in Fig. 4.

As shown in Fig. 4, the velocity of surface particulate flow in all sampling areas are accelerated first from stationary stat, then gradually decelerate after reaching their peaks which indicates that the entire surface particle flow experiences the complete avalanche process. The time of peak velocity at each sampling area is differen. The surface particulate flow at A3 reaches its peak velocity firstly at the forth slice (signed as P1 in Fig. 4), and the flows at A1 and A5 regions arrive at their peak velocities at the seventh slice (signed as P2 in Fig. 4), which is significantly lagging behind P1. The hysteresis can be interpreted that because A1 and A5 are located at the edge of the drum that is far from the initial position, the particles at the two regions avalanche later than those at other regions. There is also an interesting fact that during the avalanche, particulate velocities at A1 and A5 show similar trends and reach their peak at the same tim, which indicates that the propagation of the avalanche in mid-to-edge pattern represent distinct symmetry. In addition, we observed that the peak velocity of the surface particulate flow at A3 is lower than its counterpart at A1 and A5 regions, the possible cause is that the drum is constantly rotating during the avalanche and leads to the increasing trend of the inclined angle of the surface particulate flow. The velocity of surface particle flow will increase when the inclined angle enlarged.[12,13]

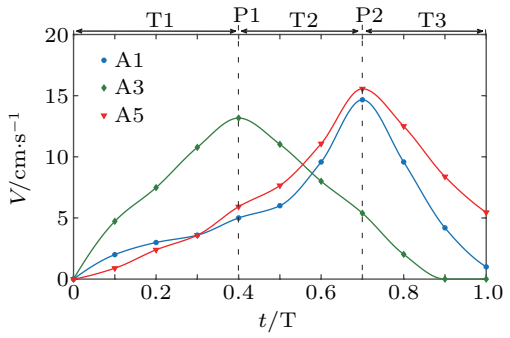


Fig. 4. The temporal distribution of velocity in mid-to-edge pattern.

To further explore that particles in the high-speed area perturb the neighboring particles along the axial direction in mid-to-edge pattern, we investigate the spatial distribution of the velocity of the surface particulate flow. In the center of the high speed are, a band region is chosen as 22 mm and 200 mm in radial and axial directions respectively. We divide this region into 12 sampling areas equally along the axial directio.As shown in Fig. 4, the whole avalanche period is divided into three segments T1, T2, and T3 respectively in accordance with P1 and P2 as dividing point. The three photographs in Fig. 2 illustrate propagation process of the avalanche in T1, T2, and T3 segments respectively. By measuring the velocity of the surface particulate flow in the sampling areas within each periodic segment, figure 5 represents the spatial distribution of the velocity of the surface particulate flow in mid-to-edge pattern. As shown in Fig. 5, the high-speed area in T1 locates at the middle of the observation area and the particle velocity is at low level due to the avalanche is in its initial stag. In T2, the high-speed area gradually moves toward the edges of the drum by constantly perturbing the adjacent particles in the axial direction. However, the particle velocities in the edge position are still low which indicates that the edge positions have not been greatly affected. The high-speed area divided into two parts and gradually move to the edges of the drum in T3 because the velocity of particles in the middle area is tend to be zero. The changes of the particle velocity clearly reveal that the high-speed area moves from the middle area to both edges of the drum, which support our previous discussion. Moreover, we focus on the propagating velocity of the avalanche in mid-to-edge pattern. By carrying the differential on the spatial distribution of the velocity of surface particulate flow and selecting the maximum and minimum of the differential values respectively, we determine the axial boundary of the high-speed region which indicates the propagation edge of the avalanche marked by the dotted line in Fig. 2. The propagating velocity of the avalanche can be indicated by the moving velocity of the propagating front of the avalanche. In addition, the T3 segment is excluded in consideration because at that time the propagating front of the avalanche has arrived at both boundaries of the observation area and its location cannot achieved accurately. As can be seen from Fig. 5, the propagating fronts of avalanche are approximately at locations 5 cm and 11.5 cm in the axial direction in the T1 segment. When the avalanche continues to T2 segment, the two propagating fronts of avalanche move to the locations 3.3 cm and 16.7 cm in the axial direction respectively. The duration of the avalanche from T1 to T2 is about 0.4 s. Thus, we can achieve the velocities of the avalanche spreads to the left and right sides in the observation area which are 4.25 cm/s and 13 cm/s respectively. We consider that the clustering of particles occurs randomly on the surface of the particle flow during the avalanche because of the particularity of the irregular particle shape, which hinders the propagation of avalanche and causes unevenness in velocity distribution.

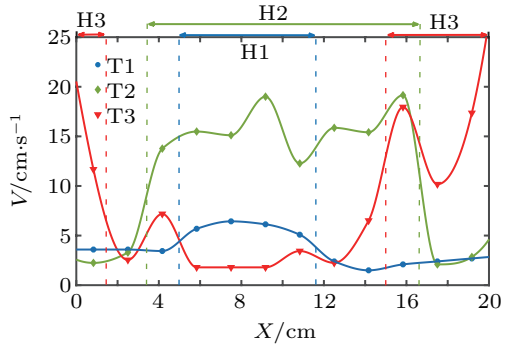


Fig. 5. The spatial distribution of velocity in mid-to-edge pattern.

3.2. Edge-to-edge pattern

Edge-to-edge pattern is another type of avalanching pattern which is different from the spherical particle. In this pattern, the avalanche is triggered at any edge areas of the drum and gradually propagates to the opposite edge along the axial direction. In the experiment, we observed that the uniform unidirectional propagating characteristics whatever the avalanche propagates from left to right or from right to left. Therefore, we analyze dynamical characteristics of the avalanches in edge-to-edge pattern by taking avalanche propagating from left to right as the case. By measuring the velocity distribution of the surface particulate flow in the observation area, we can obtain the propagation process of the edge–edge avalanching pattern as shown in Fig. 6. The high-speed area constantly perturbs the neighboring particles which result in the movement of the high-speed area. That is the avalanche keeps propagating from the left edge toward the right edge in the observation area and the particles start avalanching in order by the distance from the location of the region and the initial position. Eventually, the propagation front of the avalanche moves to the right edge of the observation area which indicates the avalanche is about to end.

We still choose 5 sampling areas marked as A1–A5 shown in Fig. 3 and divide the avalanche into 10 periodic slices to investigate the edge-to-edge pattern. By measuring the velocity of the surface particulate flow of the 5 sampling areas in each periodic slice, we obtain the temporal distribution of the edge-to-edge pattern as shown in Fig. 7. The surface particulate flows in the A1–A5 sampling areas reach their peak velocities in order by the left to right during an avalanche period, which indicates that the propagating direction of the avalanche is from the left edge to the right edge in the observation area. The velocity of surface particulate flow in each sampling area overall increases gradually. However, the velocities at A2 and A4 regions have a downward trend, the possible reason for which is the formation of the mound on the surface particulate flow and delay the propagation of the avalanche.[15] To elaborate the dynamical characteristics of the avalanche in edge-to-edge pattern, we choose P1 and P2 in which the surface particulate flows in the A2 and A4 regions reach their peak velocities respectively. As shown in Fig. 7, the avalanche period is divided into T1, T2, and T3 periodic segments in accordance with P1 and P2 as dividing points.

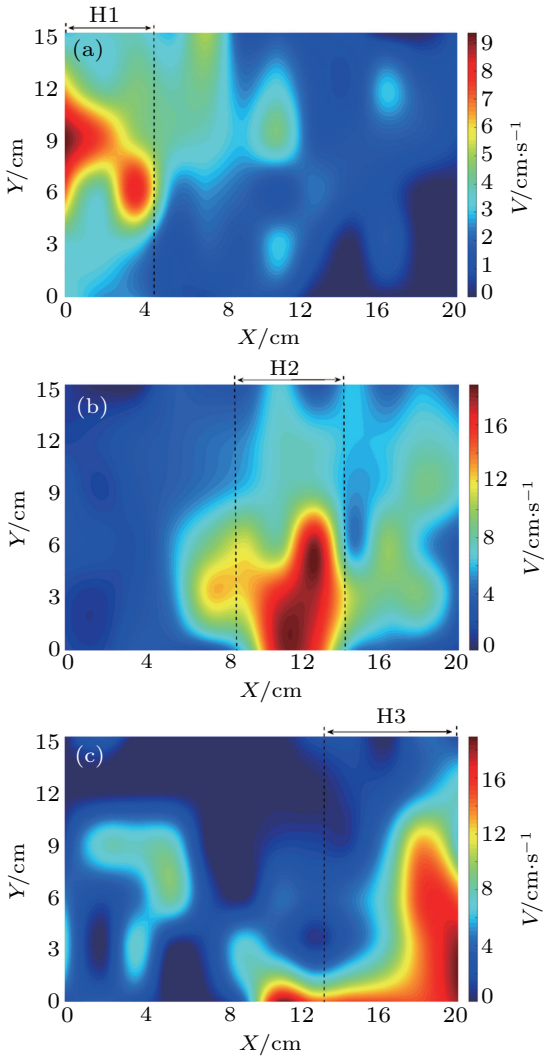


Fig. 6. The velocity distributions of the surface particulate flow in edge-to-edge pattern. (a) The velocity distribution at the initial stage, (b) the velocity distribution at the middle stage, and (c) the velocity distribution at the end stage of the avalanche.

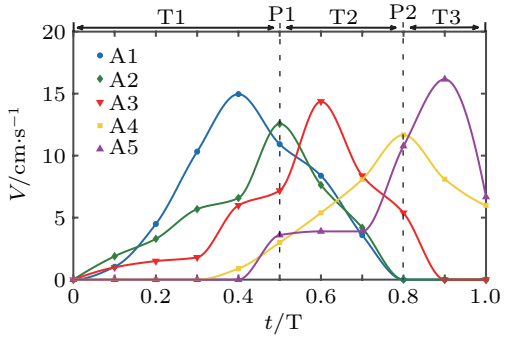


Fig. 7. The temporal distribution of velocity in edge-to-edge pattern.

To further illustrate the dynamic characteristics of surface particulate flow in edge-to-edge pattern, we use the similar method mentioned in Subsection 3.1 to obtain the spatial distribution of the velocity of the surface particulate flow in the

edge-to-edge pattern. As shown in Fig. 8, the avalanche occurs at the left edge of the observation area where the particle velocity is much higher than those at other regions in T1. By means of constantly perturbing the axial neighbors, the high-speed area gradually moves toward the right edge of the drum in T2. In the end stage of the avalanche, the high-speed area moves to the right edge.Here, we also interest in the propagating velocity of the avalanche in edge-to-edge pattern. It can be seen from Fig. 8 that the front edge of avalanche locates approximately at 3.2 cm in the axial direction in T1 segment. When the avalanche comes to T2 segment, the propagating front of avalanche moves to 1.2 cm in the axial direction. The duration of the avalanche from T1 to T2 is about 0.63 s. So, the spread velocity of the avalanche in the edge-to-edge pattern is 15.87 cm/s.

An explanation for edge-to-edge pattern can possibly process from that the upper reposing angle of irregular particles is much larger than the counterpart of the spherical particles. The effect of the edge of the drum is not sufficient to support the unstable particles when the avalanche occurs. Therefore, the avalanches of irregular particles may occur on the edge areas of the drum.

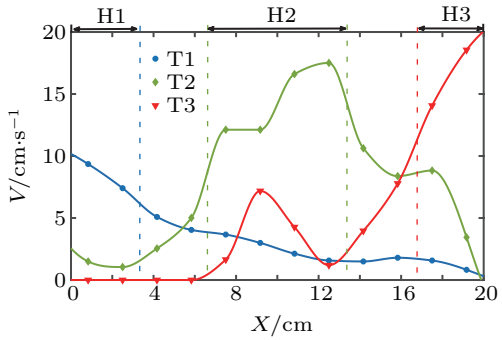


Fig. 8. The spatial distribution of velocity of the surface particulate flow in edge-to-edge pattern.

4. Conclusion

In this paper, we studied two types of interesting avalanching pattern for irregular particles in the axial direction of the rotating drum which named as mid-to-edge pattern and edge-to-edge pattern respectively. In mid-to-edge pattern which is similar to the avalanche of the spherical particles, the avalanches are initial at the middle of the drum, whereas the avalanches in edge-to-edge pattern are triggered at the edge of the drum. In our opinion, the particles in the high-speed area constantly perturb and destabilize the neighboring particles which is sufficient to make some of them into motion. The continuous repetition of the process led to the two types of avalanching pattern. Furthermore, we quantitatively investigated the temporal and spatial characteristics of these avalanching patterns and achieved the corresponding propagating velocities in the axial direction.

References

[1] Midi G D R 2004 *Eur. Phys. J. E* **14** 341
[2] Seiden G and Thomas P J 2011 *Rev. Mod. Phys.* **83** 1323
[3] Kruggel-emden H, Rickelt S, Wirtz S and Scherer V 2008 *Powder Technol.* **188** 153
[4] Cleary P W 2010 *Particuology* **8** 106
[5] Mu J and Perlmutter D D 1980 *AICHE J.* **26** 928
[6] Henein H, Brimacombe J K and Watkinson A P 1985 *Metall. Trans. B* **16** 763
[7] Pollard B L and Henein H 1989 *Can. Metall. Q.* **28** 29
[8] Woodle G R and Munro J M 1993 *Powder Technol.* **76** 241
[9] Van D R, Young B R, Wilson M A and Schmidt S J 1999 *Powder Technol.* **106** 183
[10] Pandey P and Turton R 2005 *AAPS Pharm. Sci. Tech.* **6** E237
[11] Dubé O, Alizadeh E, Chaouki J and Bertrand F 2013 *Chem. Eng. Sci.* **101** 486
[12] Mou S H, Yang H, Li R, Zhang G H, Sun Q C and Kong P 2019 *Powder Technol.* **344** 1
[13] Song J, Yang H, Li R, Chen Q, Zhang Y J, Wang Y J and Kong P 2019 *Powder Technol.* **355** 172
[14] Pan G J, Zhang D M, Yin Y P and He M H 2006 *Chin. Phys. Lett.* **23** 2811
[15] Daerr A and Douady S 1999 *Nature* **399** 241
[16] Rajchenbach J 2001 *Phys. Rev. Lett.* **88** 014301
[17] Yang H, Zhang B F, Li R, Zheng G and Zivkovic V 2017 *Powder Technol.* **311** 439
[18] Zhang Y J, Yang H, Li R, Chen Q, Sun Q C and Kong P 2019 *Powder Technol.* **355** 333
[19] Gong J M, Yang H, Lin S H, Li R and Zivkovic V 2018 *Powder Technol.* **324** 76
[20] Lin S H, Yang H, Li R, Zheng G and Zivkovic V 2018 *Powder Technol.* **338** 376
[21] Orpe A V and Khakhar D V 2007 *J. Fluid Mech.* **571** 1
[22] Hagemeier T, Roloff C, Bück A and Tsotsas E 2015 *Particuology* **22** 39
[23] Li R, Yang H, Zheng G, Zhang B F, Fei M L and Sun Q C 2016 *Powder Technol.* **295** 167
[24] Yang H, Zhu Y H, Li R and Sun Q C 2019 *Particuology* (in Press)
[25] Yang H, Jiang G L, Sawe H Y, Davies C, Biggs M J and Zivkovic V 2016 *Chem. Eng. Sci.* **149** 1
[26] Leadbeater T W, Parker D J and Gargiuli J 2012 *Particuology* **10** 146
[27] Stannarius R 2017 *Rev. Sci. Instrum.* **88** 51806
[28] Bergeler S and Krambeer H 2004 *Meas. Sci. Technol.* **15** 1309
[29] Ator J T 1963 *J. Opt. Soc. Am.* **53** 1416
[30] Uddin M S, Inaba H, Itakura Y and Kasahara M 1998 *Appl. Opt.* **37** 6234
[31] Aizu Y and Asakura T 2006 *Spatial Filtering Velocimetry: Fundamentals And Applications*, Vol. 116 (Newtherlands: Springer Science & Business Media)
[32] Xu C, Zhou B, Yang D, Tang G and Wang S 2008 *Meas. Sci. Technol.* **19** 024005
[33] Li J, Xu C and Wang S 2014 *Meas. J. Int. Meas. Confed.* **53** 194